Synthetic graphene in real bilayers and synthetic bilayers of real graphene

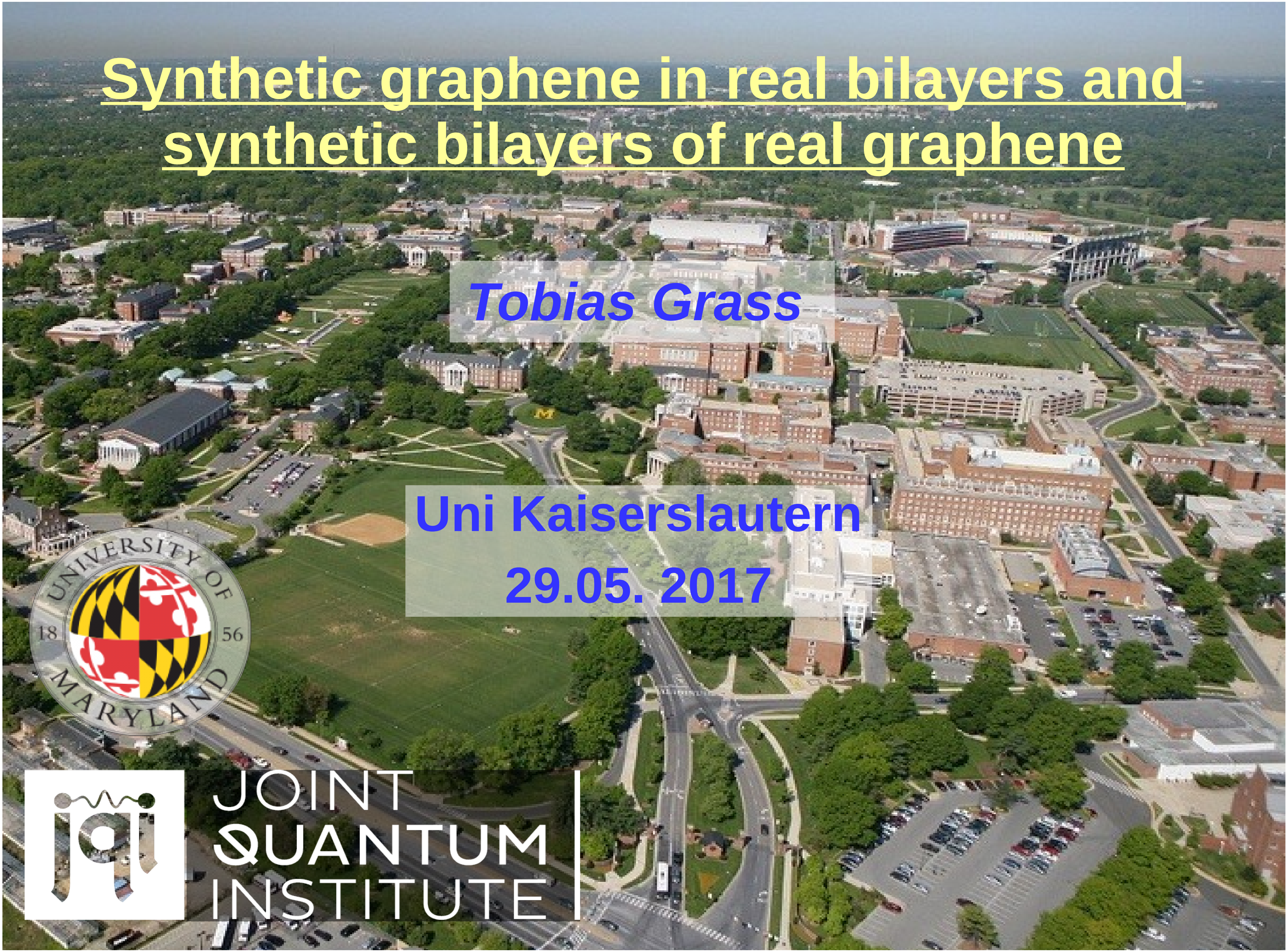

Tobias Grass

Uni Kaiserslautern

29.05. 2017

UNIVERSITY OF MARYLAND 18 56

JOINT QUANTUM INSTITUTE

First part: Artificial graphene / real bilayer

Work published in:
2D Mater. 4 (2017) 015039

Ravindra Chhajlany

(U Poznan)

Leticia Tarruell

Maciej Lewenstein

(ICFO)

Vittorio Pellegrini

(IIT Genova)

Second part: Real graphene / artificial bilayer

Work in progress!

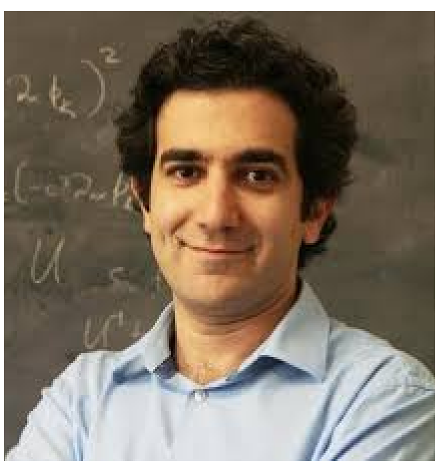

Mohammad Hafezi

Michael Gullans

(JQI / NIST)

Areg Ghazaryan

Pouyan Ghaemi

(City College New York)

First part:

Artificial graphene / real bilayer

Why to build a bilayer?

- Coulomb drag
  [cf. B. N. Narozhny and A. Levchenko, Rev. Mod. Phys. 88, 025003 (2016)]

  with two layers of graphene
  [e.g. Gorbachev, R. V. *et al. (Manchester)* Strong Coulomb drag and broken symmetry in double-layer graphene. Nat. Phys. **8**, 896 (2012)]

  or two layers of non-relativistic 2DEG

  or heterostructures (graphene + 2DEG)
  [see figure]

- Single-particle effects when combining graphene and hexagonal boron nitride

  [Yankowitz, M. *et al. (Tucson)* Emergence of superlattice Dirac points in graphene on hexagonal boron nitride. Nat. Phys. **8**, 382 (2012)]

Let's see what we can do with artificial graphene…

From
Anomalous low-temperature Coulomb drag in graphene-GaAs heterostructures
A. Gamucci, D. Spirito, M. Carrega, B. Karmakar, A. Lombardo, M. Bruna, L. N. Pfeiffer, K. W. West, A. C. Ferrari, M. Polini & V. Pellegrini
Nature Communications **5**, Article number: 5824 | doi:10.1038/ncomms6824

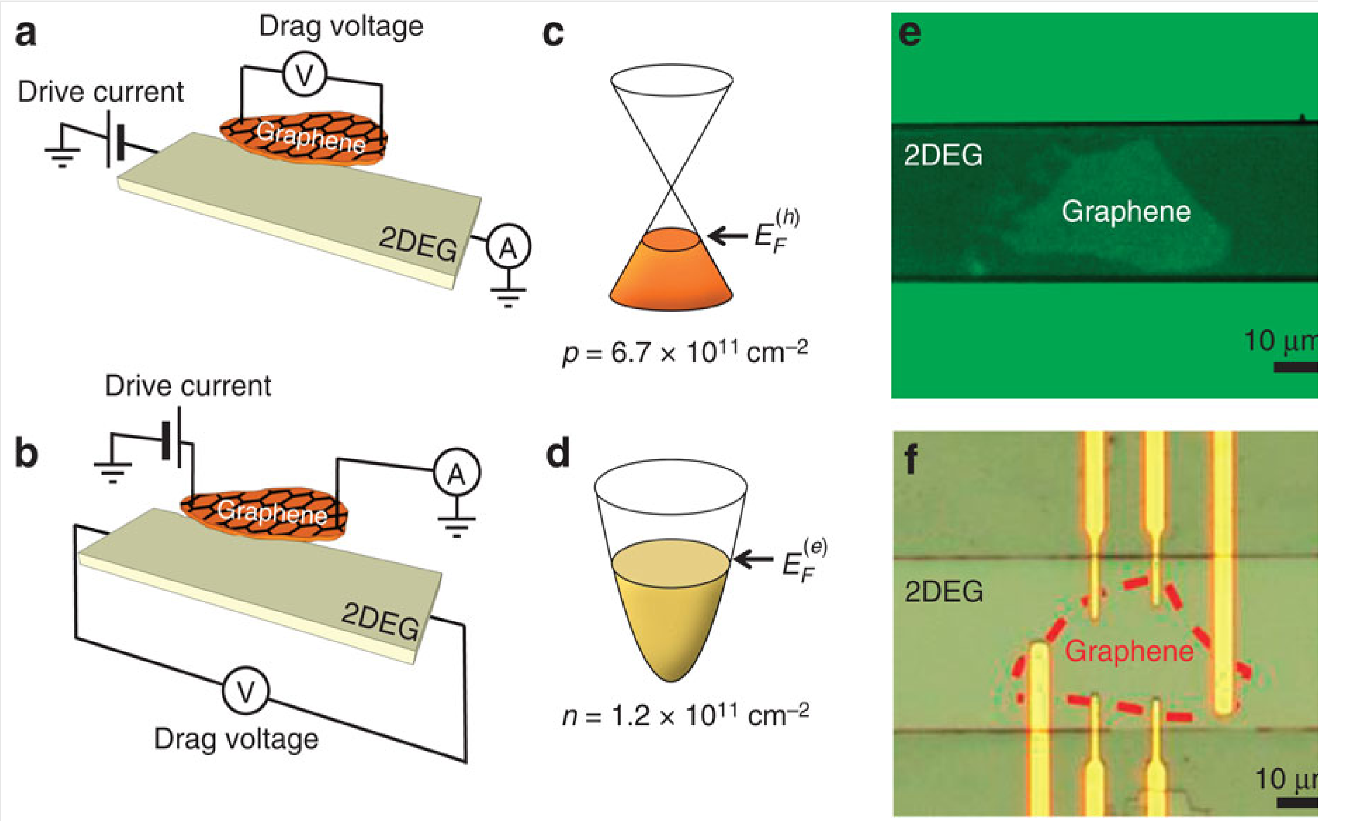

(**a**,**b**) Configurations for the Coulomb drag measurements. In **a**, a voltage drop V_{drag} appears in graphene, in response to a drive current I_{drive} flowing in the 2DEG. In **b**, the opposite occurs. The drag voltage is measured with a low-noise voltage amplifier coupled to a voltmeter as a function of the applied bias. The drive current is also monitored. (**c**) Conical massless Dirac fermion band structure of low-energy carriers in SLG. The SLG in this work is hole-doped. (**d**) Parabolic band structure of ordinary Schrödinger electrons in the 2DEG. (**e**) Optical micrograph of the device before the deposition of Ohmic contacts. The SL flake becomes visible in green light after the sample is coated with a polymer (PMMA)[31]. The scale bar is 10 μm long. (**f**) Optical microscopy image of the contacted SLG on the etched 2DEG GaAs channel. The red dashed line denotes the SLG boundaries. The scale bar is 10 μm long.

Artificial graphene

Subject particles to hexagonal lattice potential!

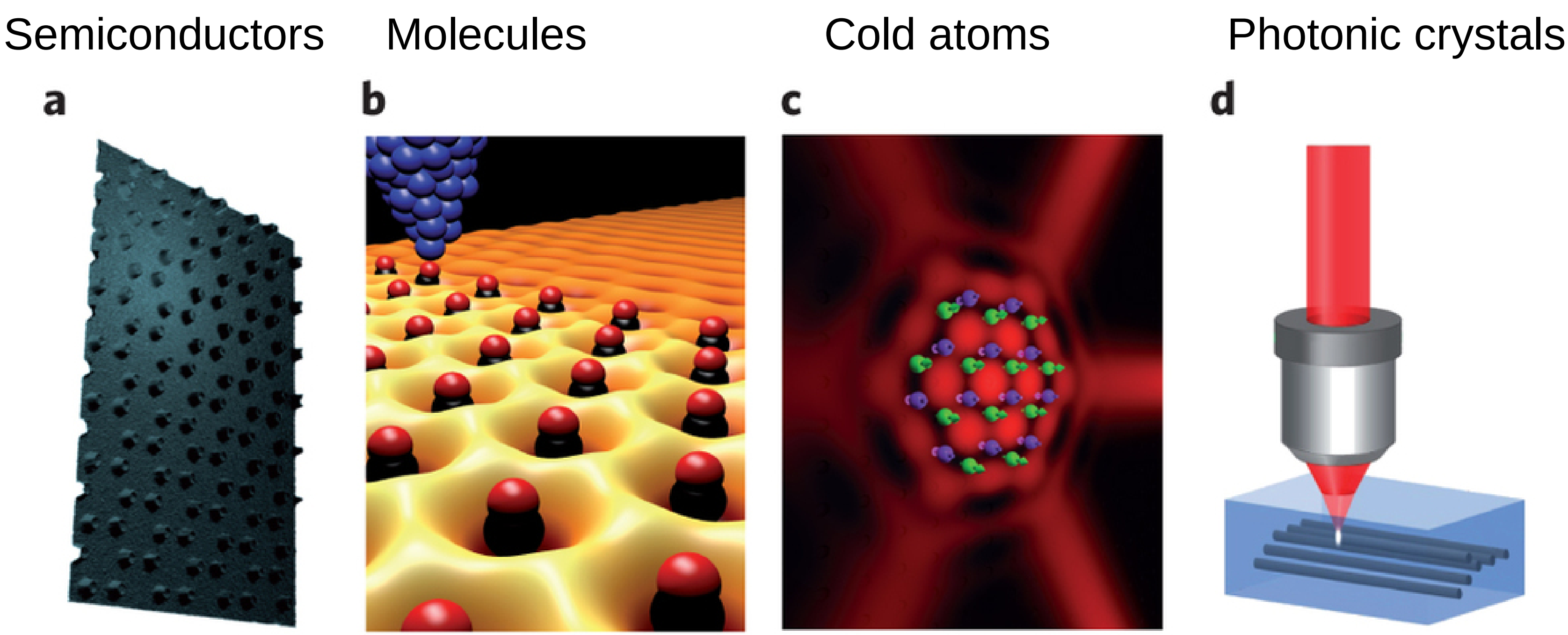

Semiconductors	Molecules	Cold atoms	Photonic crystals
$V_0 \approx 10$ K	$V_0 \approx 10^3$ K	$V_0 \approx 10$ mK	$\Delta n \approx 10^{-3}$
$d \approx 20$–100 nm	$d \approx 1$–3 nm	$d \approx 500$ nm	$d \approx 10$ μm–10 mm
$N \approx 10$–10^7	$N \approx 10^2$–10^3	$N \approx 10^5$	$N \approx 10$–10^3
$U \approx 10$ K	$U \approx 600$ K	$U \approx 100$ nK	n/a
$V \approx 1$ K	$V << U$	$V << U$	n/a
$t \approx 1$–10 K	$t \approx 10^3$ K	$t \approx 0.1$–10^3 nK	$c_0 \approx$ cm^{-1}
$T_F \approx 0.1$–100 K	$T_F \approx 5$–500 K	$T_F \approx 100$ nK	n/a

From review article: Marco Polini *et al.* , Artificial honeycomb lattices for electrons, atoms and photons, Nat. Nano 8, 625 (2013)

Cold atom artificial graphene

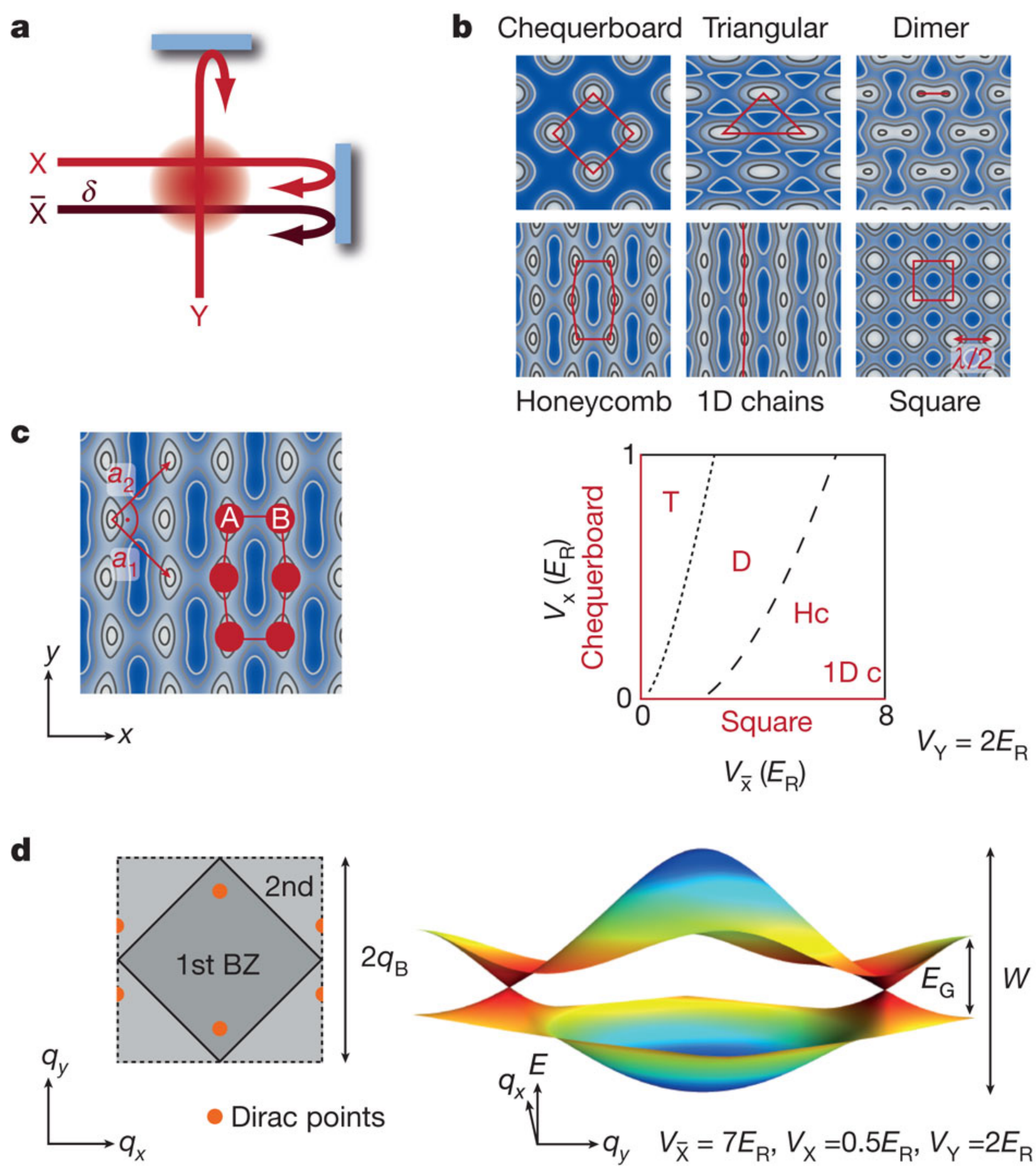

[Leticia Tarruell *et al.* Creating, moving and merging Dirac points with a Fermi gas in a tunable honeycomb lattice. Nature 483, 302 (2012)]

Bilayer setup

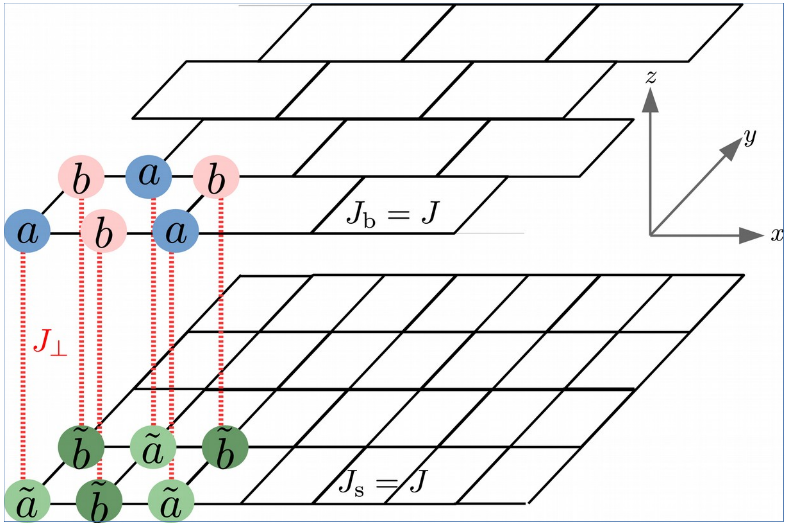

Graphene layer on top of “normal” layer:
Combine brick-wall lattice and square lattice!

Bilayer setup

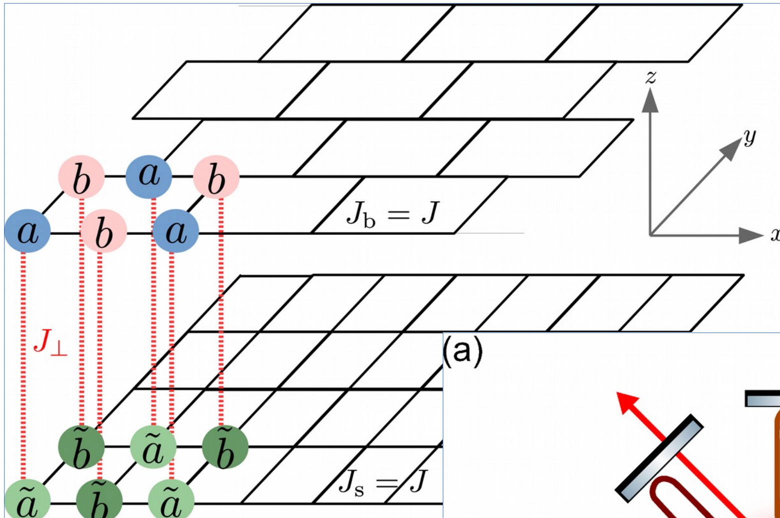

Graphene layer on top of "normal" layer:
Combine brick-wall lattice and square lattice!

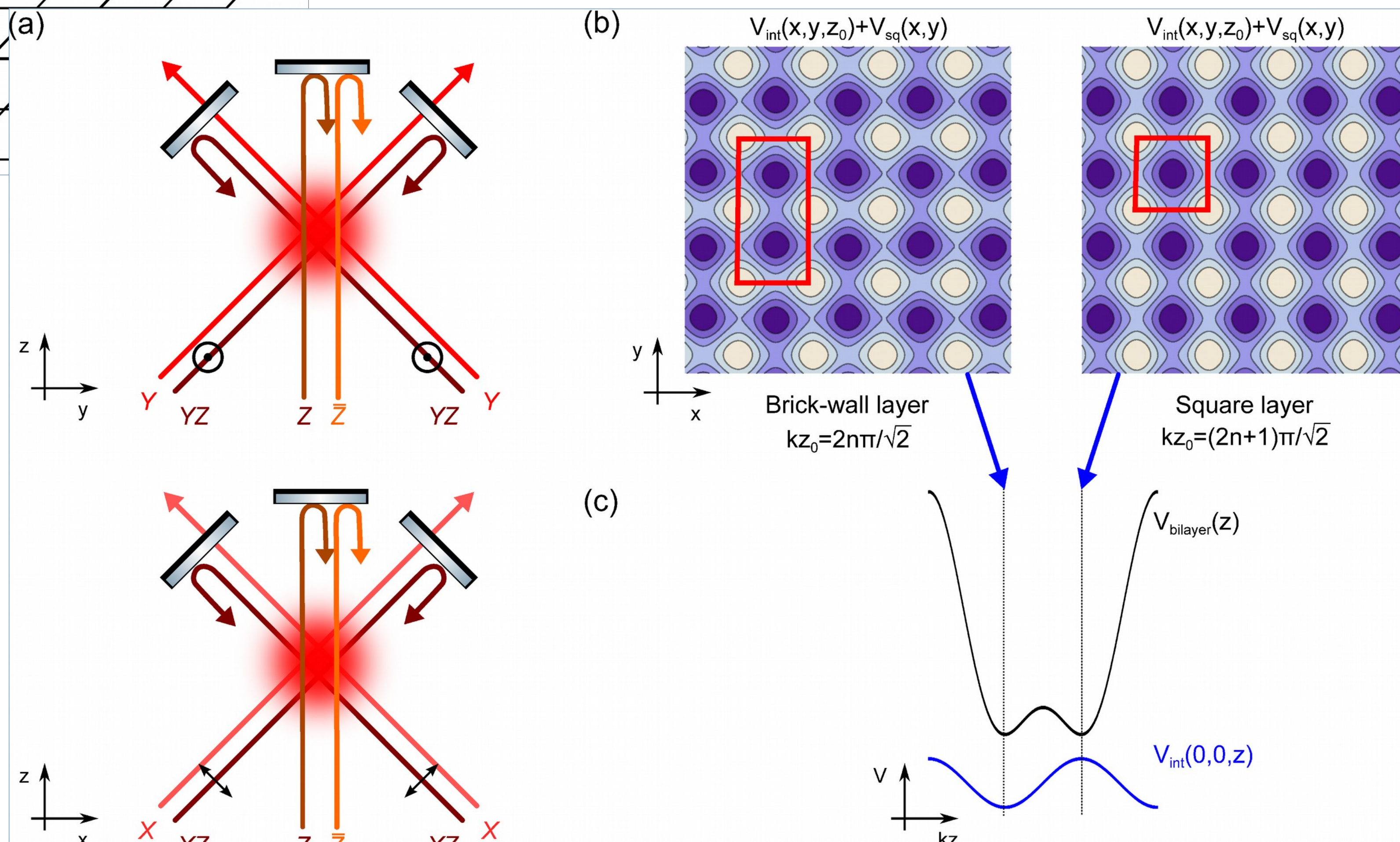

Possible with depicted arrangement of ten laser beams.

Bandstructure in the bilayer

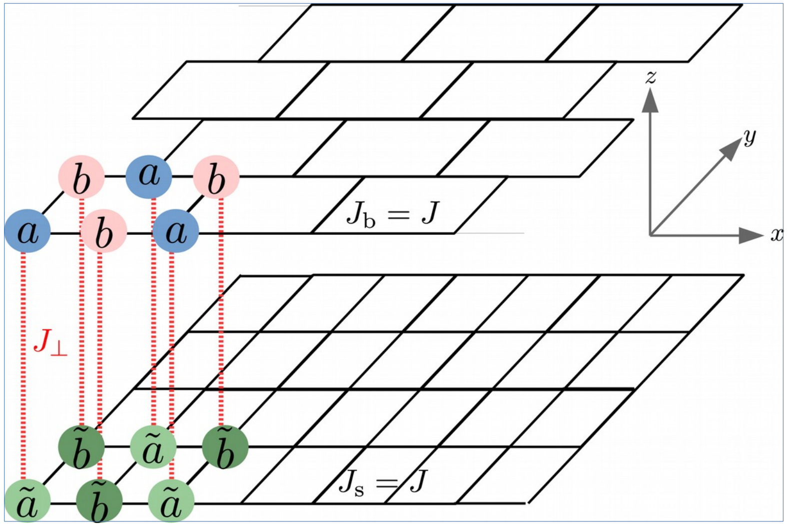

Tight-binding Hamiltonian:

$$H_\mathrm{tb} = -\,J_\mathrm{b}\sum_{\mathbf{i}\in A}\left(b^\dagger_{\mathbf{i}+\hat{x}}a_\mathbf{i} + b^\dagger_{\mathbf{i}-\hat{x}}a_\mathbf{i} + b^\dagger_{\mathbf{i}+\hat{y}}a_\mathbf{i}\right) - J_\mathrm{s}\sum_{\langle\mathbf{i},\mathbf{j}\rangle}\tilde{b}^\dagger_\mathbf{j}\tilde{a}_\mathbf{i} - J_\perp\sum_\mathbf{i}\left(a^\dagger_\mathbf{i}\tilde{a}_\mathbf{i} + b^\dagger_\mathbf{i}\tilde{b}_\mathbf{i}\right) + \mathrm{H.c.},$$

Uncoupled bands:

$$E_\pm(\mathbf{k}) = \pm\,E_\mathrm{br}(\mathbf{k}) = \pm J\sqrt{3 + 2\cos(2k_x a) + 2\cos[(k_x + k_y)a] + 2\cos[(k_x - k_y)a]},$$

$$E_\mathrm{sq}(\mathbf{k}) = -\,2J\,[\cos(k_x a) + \cos(k_y a)]\,,$$

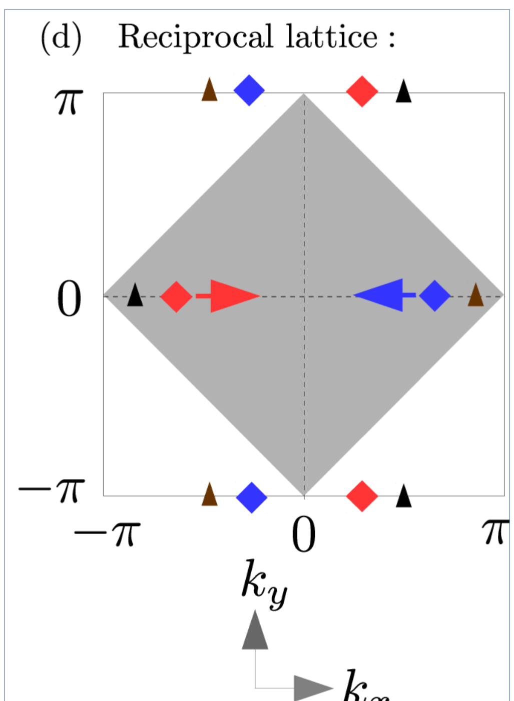

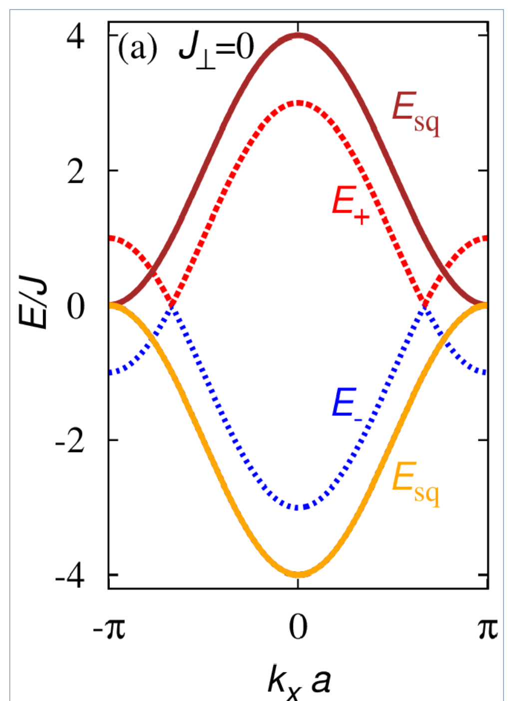

Bandstructure in the bilayer

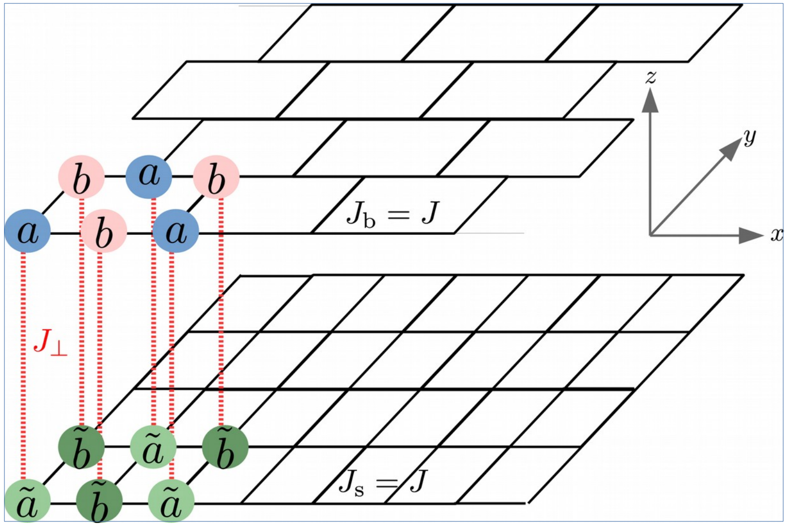

Tight-binding Hamiltonian:

$$H_{\rm tb} = -J_{\rm b} \sum_{\mathbf{i}\in A} \left(b^\dagger_{\mathbf{i}+\hat{x}} a_{\mathbf{i}} + b^\dagger_{\mathbf{i}-\hat{x}} a_{\mathbf{i}} + b^\dagger_{\mathbf{i}+\hat{y}} a_{\mathbf{i}} \right) - J_{\rm s} \sum_{\langle \mathbf{i},\mathbf{j}\rangle} \tilde{b}^\dagger_{\mathbf{j}} \tilde{a}_{\mathbf{i}} - J_\perp \sum_{\mathbf{i}} \left(a^\dagger_{\mathbf{i}} \tilde{a}_{\mathbf{i}} + b^\dagger_{\mathbf{i}} \tilde{b}_{\mathbf{i}} \right) + \mathrm{H.c.}$$

- Interlayer coupling generates new Dirac points at intersections of square-layer band and brick-wall layer band.
- Interlayer coupling shifts graphene Dirac points towards the BZ center where they finally merge.

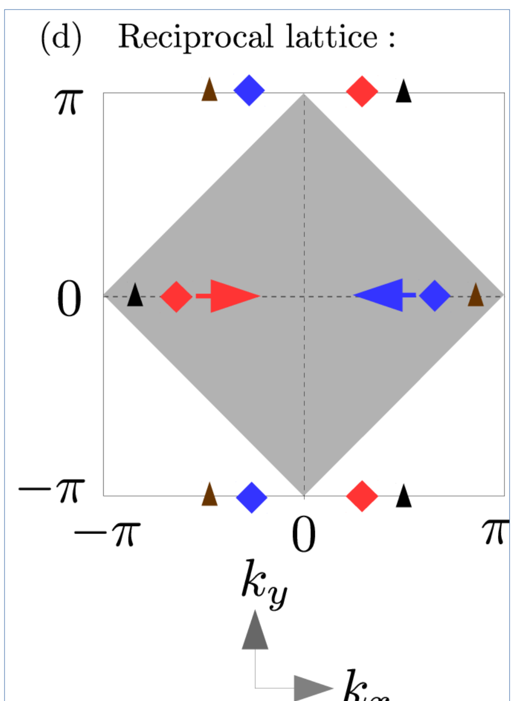

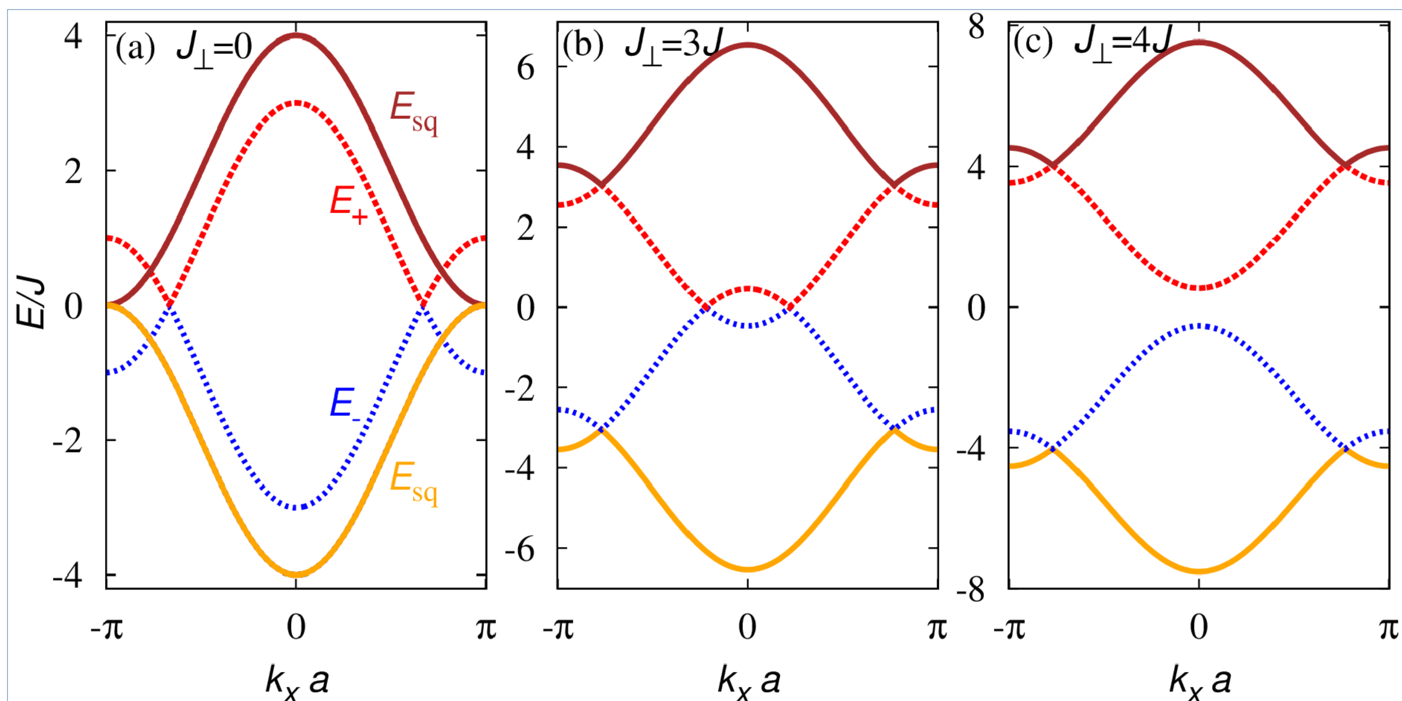

A curiosity: Bandstructure at merging point

Excitations characterized by gap, velocity, effective mass:

$$E(k) \sim \Delta + \hbar v k + \frac{\hbar^2 k^2}{2m} + \dots$$

Along the two in-plane directions, excitations look very differently when Dirac points merge:
Coexistence of massless and massive excitations!

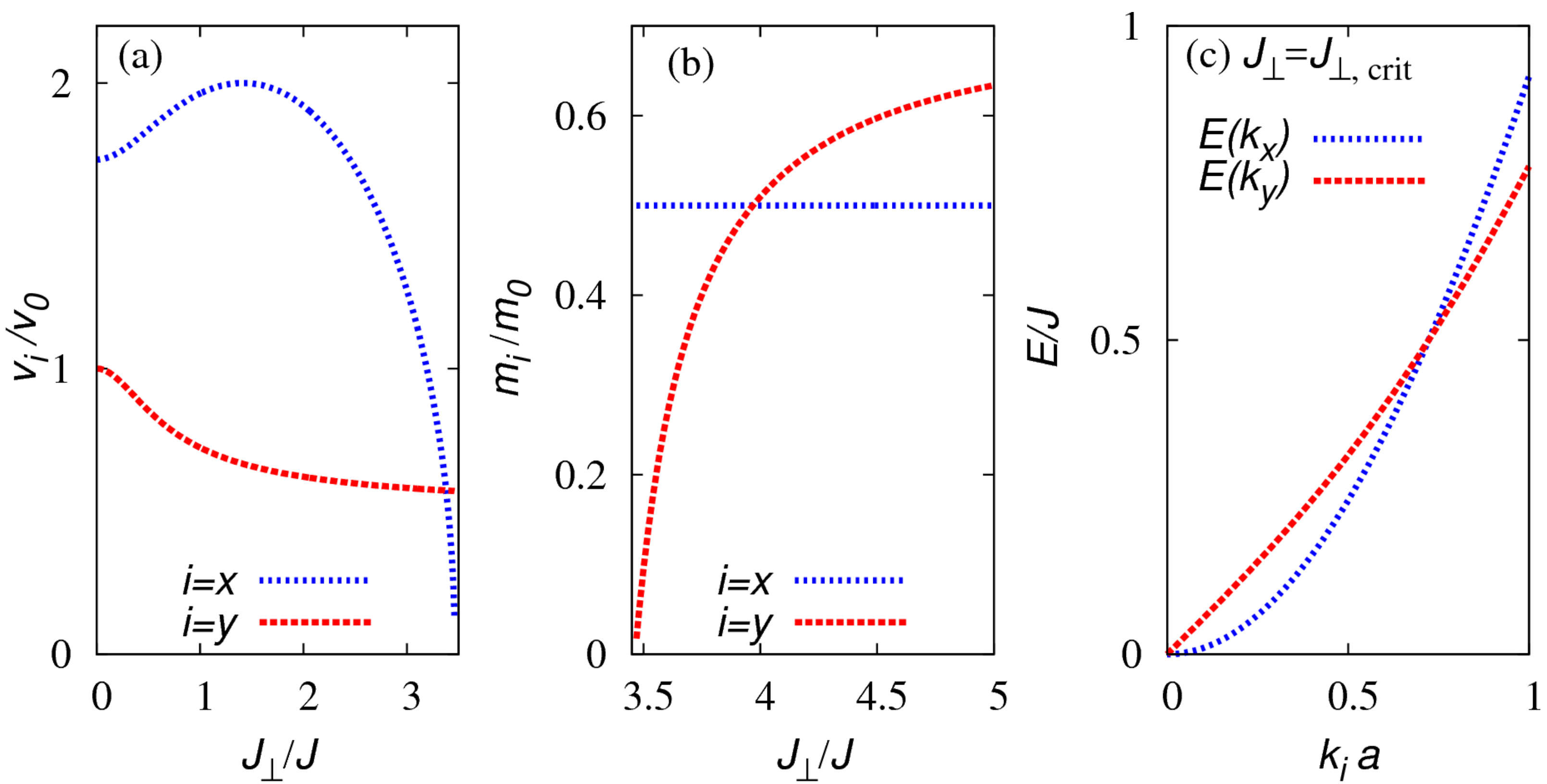

See also:
G. Montambaux, F. Piéchon, J.-N. Fuchs, and M. O. Goerbig, Phys. Rev. B 80, 153412 (2009)
P. Dietl, F. Piéchon, and G. Montambaux, Phys. Rev. Lett. 100, 236405 (2008)

Mean-field for attractive interactions

Fill bilayer with spin-1/2 fermions → interactions on doubly occupied sites:

$$H_{\rm int} = U\sum_{\mathbf{i}}(a^\dagger_{\mathbf{i}\uparrow}a^\dagger_{\mathbf{i}\downarrow}a_{\mathbf{i}\downarrow}a_{\mathbf{i}\uparrow} + b^\dagger_{\mathbf{i}\uparrow}b^\dagger_{\mathbf{i}\downarrow}b_{\mathbf{i}\downarrow}b_{\mathbf{i}\uparrow} + \tilde{a}^\dagger_{\mathbf{i}\uparrow}\tilde{a}^\dagger_{\mathbf{i}\downarrow}\tilde{a}_{\mathbf{i}\downarrow}\tilde{a}_{\mathbf{i}\uparrow} + \tilde{b}^\dagger_{\mathbf{i}\uparrow}\tilde{b}^\dagger_{\mathbf{i}\downarrow}\tilde{b}_{\mathbf{i}\downarrow}\tilde{b}_{\mathbf{i}\uparrow}),$$

Mean-field decoupling for attractive interactions (*U=-u<0*):

$$\Delta_{\rm br} \equiv (4u/N)\sum_{\mathbf{k}}\langle a_{-\mathbf{k}\downarrow}a_{\mathbf{k}\uparrow}\rangle = (4u/N)\sum_{\mathbf{k}}\langle b_{-\mathbf{k}\downarrow}b_{\mathbf{k}\uparrow}\rangle, \qquad \Delta_{\rm sq} \equiv (4u/N)\sum_{\mathbf{k}}\langle \tilde{a}_{-\mathbf{k}\downarrow}\tilde{a}_{\mathbf{k}\uparrow}\rangle = (4u/N)\sum_{\mathbf{k}}\langle \tilde{b}_{-\mathbf{k}\downarrow}\tilde{b}_{\mathbf{k}\uparrow}\rangle.$$

Quadratic Hamiltonian:

$$H_{\rm BCS} = \sum_{\sigma\neq\sigma'}\sum_{\mathbf{k}}\left(a^\dagger_{\mathbf{k}\sigma}, a_{-\mathbf{k}\sigma'}, b^\dagger_{\mathbf{k}\sigma}, b_{-\mathbf{k}\sigma'}, \tilde{a}^\dagger_{\mathbf{k}\sigma}, \tilde{a}_{-\mathbf{k}\sigma'}, \tilde{b}^\dagger_{\mathbf{k}\sigma}, \tilde{b}_{-\mathbf{k}\sigma'}\right)\cdot\begin{pmatrix} -\mu & \Delta_{\rm br} & -J^{\rm br}_{\mathbf{k}} & 0 & -J_\perp & 0 & 0 & 0 \\ \Delta^*_{\rm br} & \mu & 0 & J^{\rm br}_{\mathbf{k}} & 0 & J_\perp & 0 & 0 \\ -J^{\rm br}_{-\mathbf{k}} & 0 & -\mu & \Delta_{\rm br} & -0 & 0 & -J_\perp & 0 \\ 0 & J^{\rm br}_{-\mathbf{k}} & \Delta^*_{\rm br} & \mu & 0 & 0 & 0 & J_\perp \\ -J_\perp & 0 & 0 & 0 & -\mu & \Delta_{\rm sq} & -J^{\rm sq}_{\mathbf{k}} & 0 \\ 0 & J_\perp & 0 & 0 & \Delta^*_{\rm sq} & \mu & 0 & J^{\rm sq}_{\mathbf{k}} \\ 0 & 0 & -J_\perp & 0 & -J^{\rm sq}_{\mathbf{k}} & 0 & -\mu & \Delta_{\rm sq} \\ 0 & 0 & 0 & J_\perp & 0 & J^{\rm sq}_{\mathbf{k}} & \Delta^*_{\rm sq} & \mu \end{pmatrix}\cdot\begin{pmatrix} a_{\mathbf{k}\sigma} \\ a^\dagger_{-\mathbf{k}\sigma'} \\ b_{\mathbf{k}\sigma} \\ b^\dagger_{-\mathbf{k}\sigma'} \\ \tilde{a}_{\mathbf{k}\sigma} \\ \tilde{a}^\dagger_{-\mathbf{k}\sigma'} \\ \tilde{b}_{\mathbf{k}\sigma} \\ \tilde{b}^\dagger_{-\mathbf{k}\sigma'} \end{pmatrix}$$

Self-consistent solution:

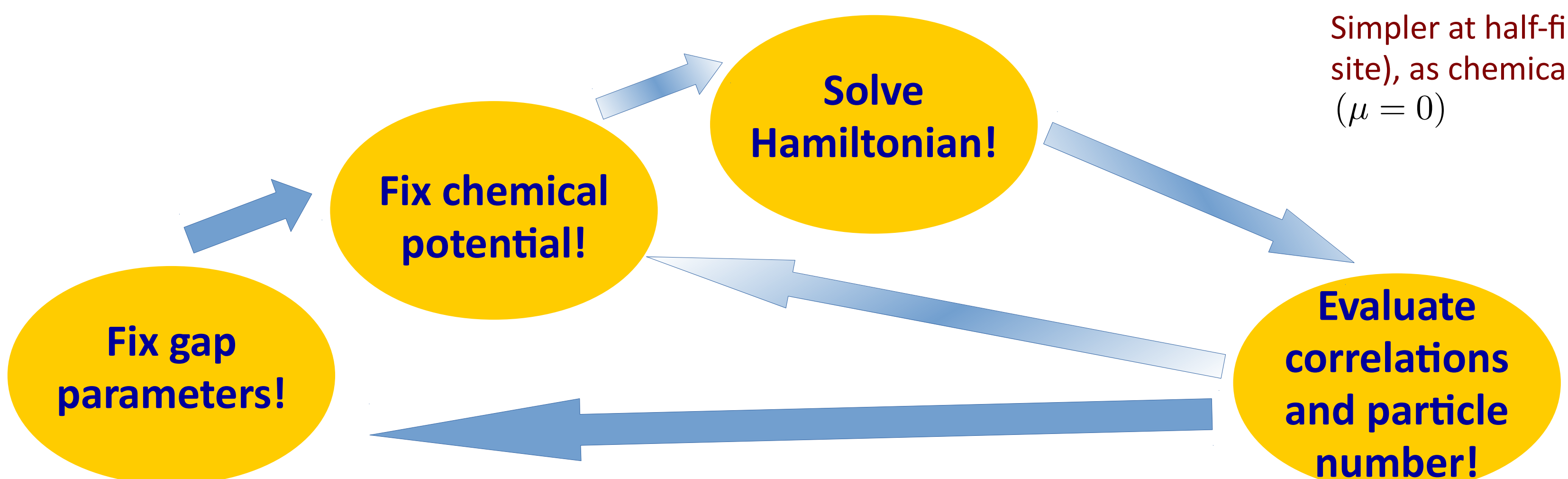

Simpler at half-filling (one atom per site), as chemical potential is fixed: $(\mu = 0)$

Superfluid vs. semimetal

Half-filling (1 atom per site):

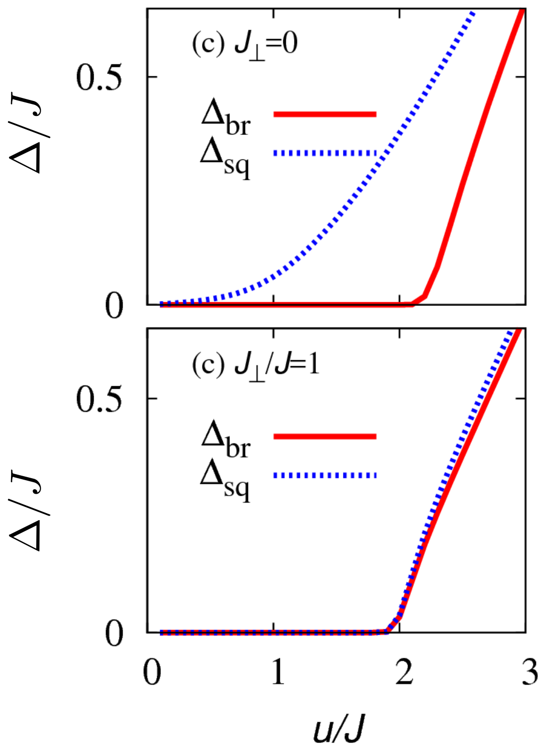

Uncoupled brick-wall layer exhibits SM-SF transition.

For weak interactions, interlayer coupling suppresses SF in square layer.

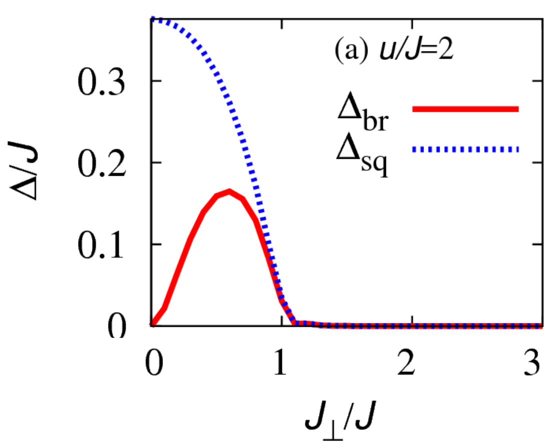

For intermediate interactions, coupling enhances SF in brick-wall layer.
Strong coupling suppresses SF in both layers.

Superfluid vs. semimetal

Half-filling (1 atom per site):

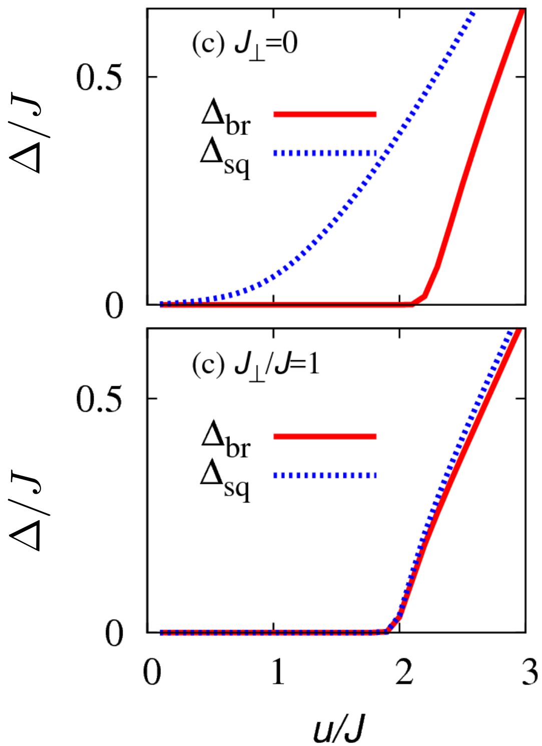

Uncoupled brick-wall layer exhibits SM-SF transition.

For weak interactions, interlayer coupling suppresses SF in square layer.

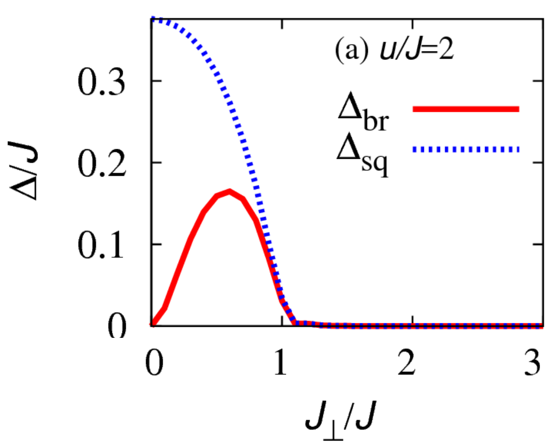

For intermediate interactions, coupling enhances SF in brick-wall layer.
Strong coupling suppresses SF in both layers.

1/4-filling (half atom per site):

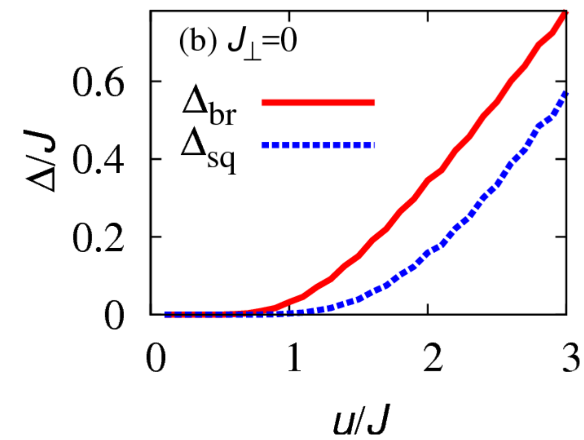

No SM phase in uncoupled system

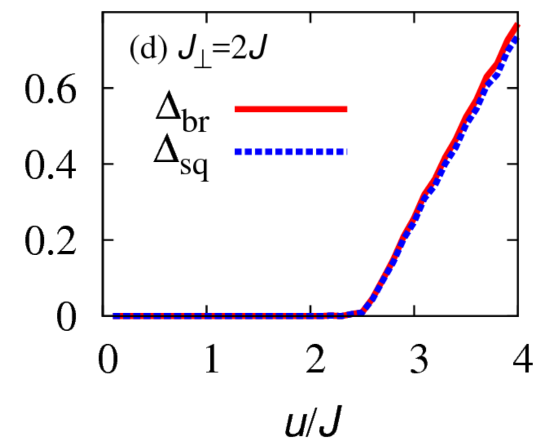

SM-SF transition at finite coupling

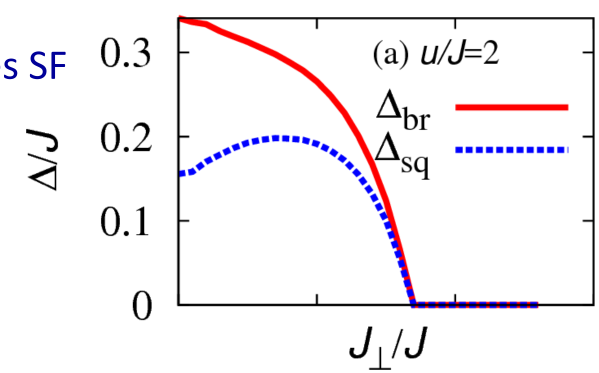

Strong coupling suppresses SF phase

Quantum magnetism

Effective Hamiltonian for strongly repulsive system: $$H_{\text{eff}} = \sum_{ij} J_{ij}^{\text{ex}} \mathbf{S}_i \cdot \mathbf{S}_j \quad \text{with} \quad J_{ij}^{\text{ex}} = J_{ij}^2/U$$

Neel-to-dimer transition upon increasing interlayer coupling:

The staggered magnetization vanishes in both layers simultaneously for $g_{\text{crit}} = \frac{J_\perp}{J} \approx 2.2$

(QMC data for up to 1152 sites)

$$S(\pi,\pi) = \langle m_{\text{s}}^2 \rangle$$

$$m_{\text{s}} = \frac{1}{N_{\text{sites}}} \left(\sum_{i\in A} \mathbf{S}_i - \sum_{i \in B} \mathbf{S}_i \right)$$

Two square layers: $g_{\text{crit}} \approx 2.5$

Two hexagonal layers: $g_{\text{crit}} \approx 1.6$

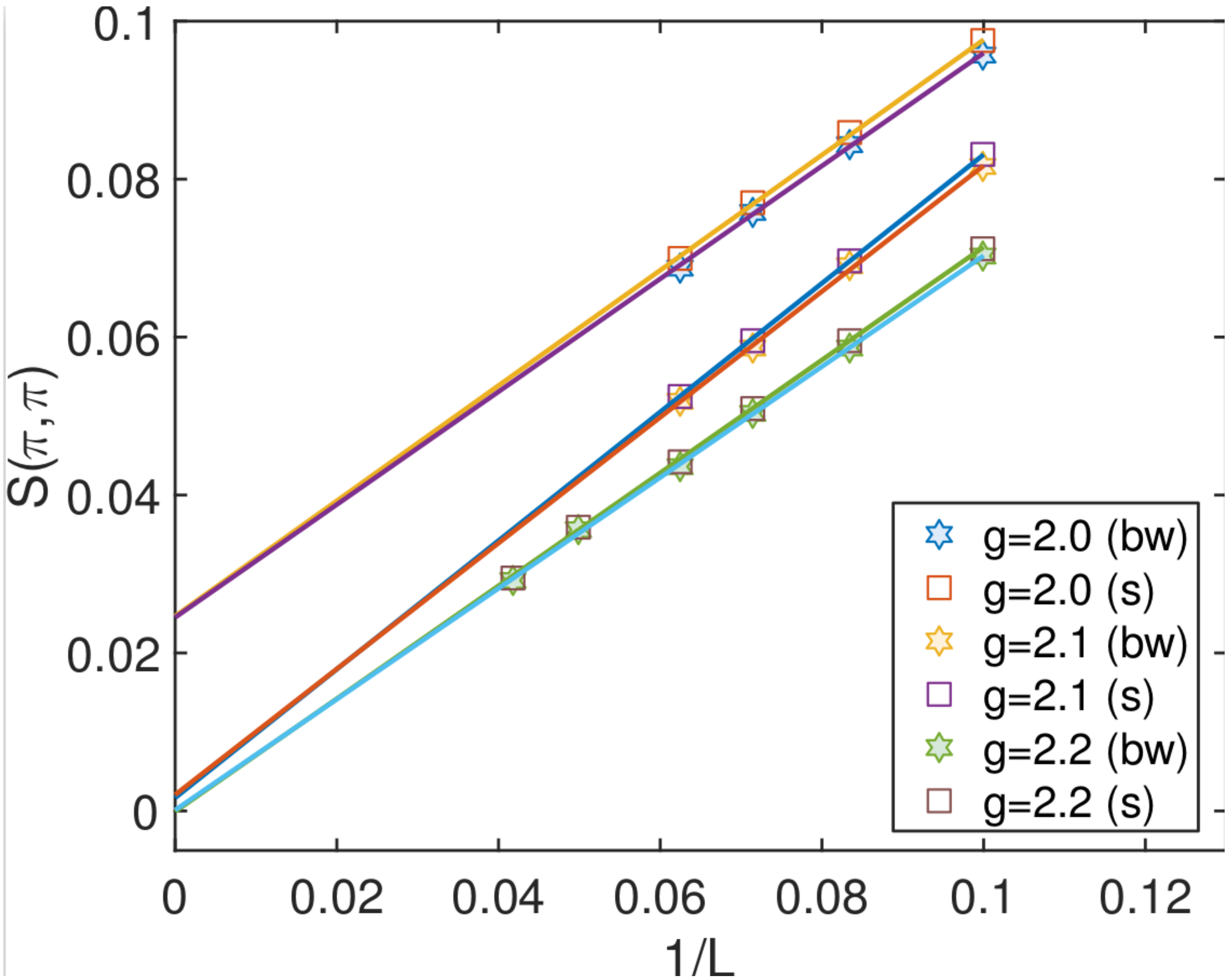

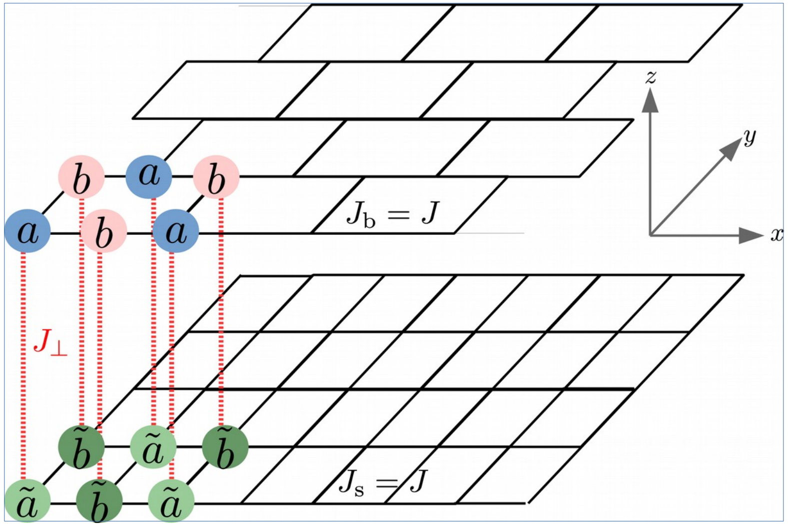

Summary …

- Shift and merge Dirac points by layer coupling!

- New Dirac points!
- Give rise to SM-SF transition at filling one-fourth.
- Interlayer coupling can enhance or suppress SF phase.

- Magnetic transition in Mott phase:
  long-range Neel to dimer.

… and Outlook

- What happens when one layer becomes topological?
  Proximity-induced topological order?
  → Haldane model
  → shaken gauge field

- Quantum magnetism with anisotropic coupling strengths: competition between dimer phase in brick-wall and long-range ordered phase in square lattice

- Mott transition in the bilayer?

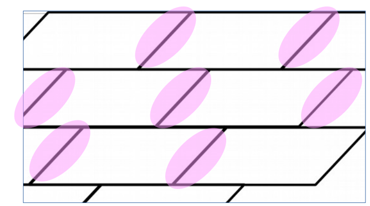

Unique dimer order in brick-wall…

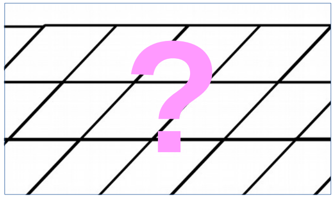

… but no corresponding order in the square lattice

Second part:

Real Graphene / Artificial Bilayer

More precisely:

Light-controlled Fractional Quantum Hall Effect in Graphene

Quantum Hall Effect

As transport phenomenon: Quantized Hall Resistance

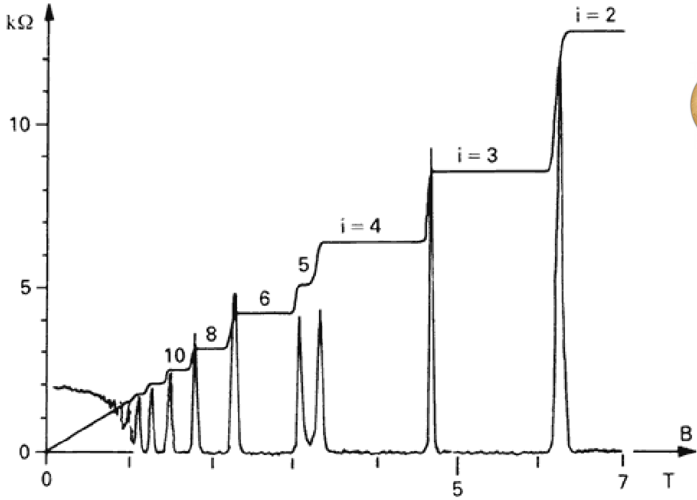

1985

Klaus v. Klitzing

Explanation in terms of topology: Protected Edge States

2016

David Thouless

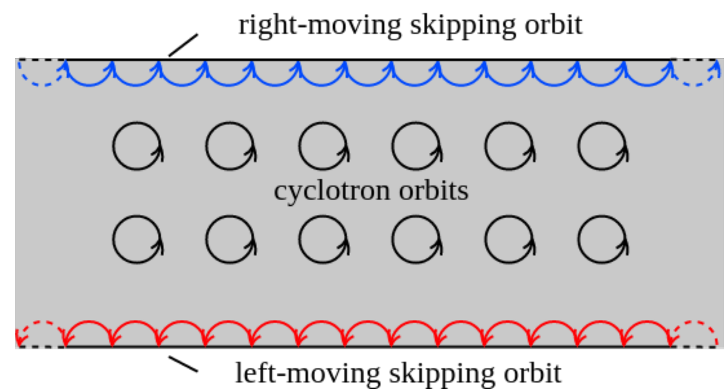

Fractional Quantum Hall Effect and Anyonic Quasiparticles

$$\Psi_{\text{Laughlin}} = \prod_{i<j}(z_i - z_j)^{1/\nu} \mathrm{e}^{-\sum_i |z_i|^2/4}$$

1998

Robert B. Laughlin
Prize share: 1/3

Horst L. Störmer
Prize share: 1/3

Daniel C. Tsui
Prize share: 1/3

Non-Abelian Anyons and Topological Quantum Computing

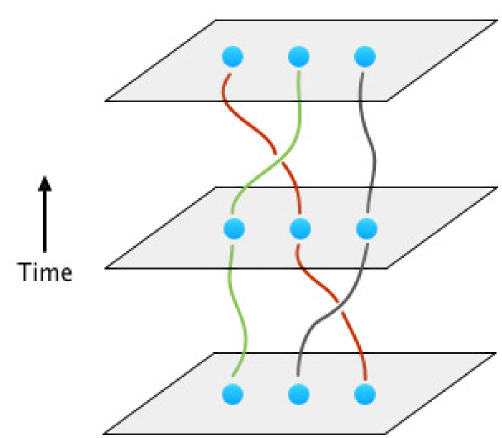

Use non-Abelian anyons as robust quantum memory.
Quantum information is processed by braiding these anyons.

NO NOBEL PRIZE YET!!

Graphene in magnetic field: Landau levels

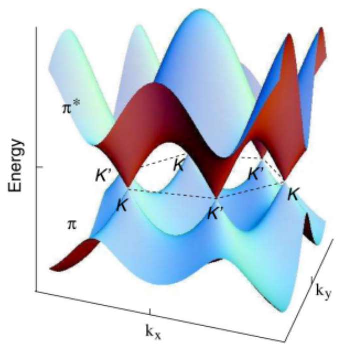

Effective Hamiltonian around Dirac point:

$$H_\xi = \xi v_{\mathrm{F}}(p_x\sigma_x + p_y\sigma_y)$$

$$\xi = \pm \text{ for } K, K'$$

Pauli matrices represent sublattice structure!

Features of relativistic Landau levels:

- Spinor wave function
- Spin and valley degeneracy: 4 bands per energy level
- Particle-hole symmetry
- Non-equidistant energy levels!

In magnetic field:

$$p_i \to \Pi_i = p_i + eA_i$$

$$\Pi_x = \frac{\hbar}{\sqrt{2}l_{\mathrm{B}}}(a^\dagger + a) \text{ and } \Pi_y = \frac{\hbar}{i\sqrt{2}l_{\mathrm{B}}}(a^\dagger - a)$$

$$H_\xi = \xi\sqrt{2}\frac{\hbar v_{\mathrm{F}}}{l_{\mathrm{B}}}\begin{pmatrix} 0 & a \\ a^\dagger & 0 \end{pmatrix}$$

"Standard" Landau level wave functions:

$$a^\dagger \varphi_{n,m} = \varphi_{n+1,m}$$

Graphene Landau level wave functions:

$$\Psi_{n=0,m} = \begin{pmatrix} 0 \\ \varphi_{0,m} \end{pmatrix} \quad \text{and} \quad \Psi_{n>0,m} = \frac{1}{\sqrt{2}}\begin{pmatrix} \varphi_{n-1,m} \\ \xi\lambda\varphi_{n,m} \end{pmatrix}$$

$$\lambda = \pm$$

At energies $$\epsilon_{\lambda n} = \lambda\frac{\hbar v_{\mathrm{F}}}{l_{\mathrm{B}}}\sqrt{2n}$$

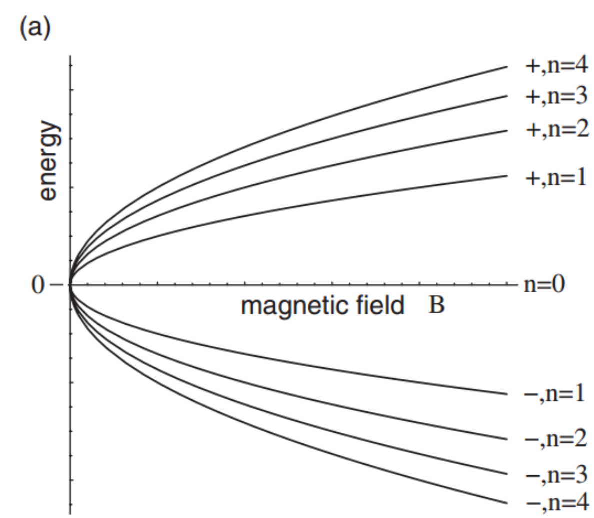

See also review article: M. Goerbig, *Electronic properties of graphene in a strong magnetic field*, Rev. Mod. Phys. **83** 4 (2011)

Optical coupling of graphene Landau levels

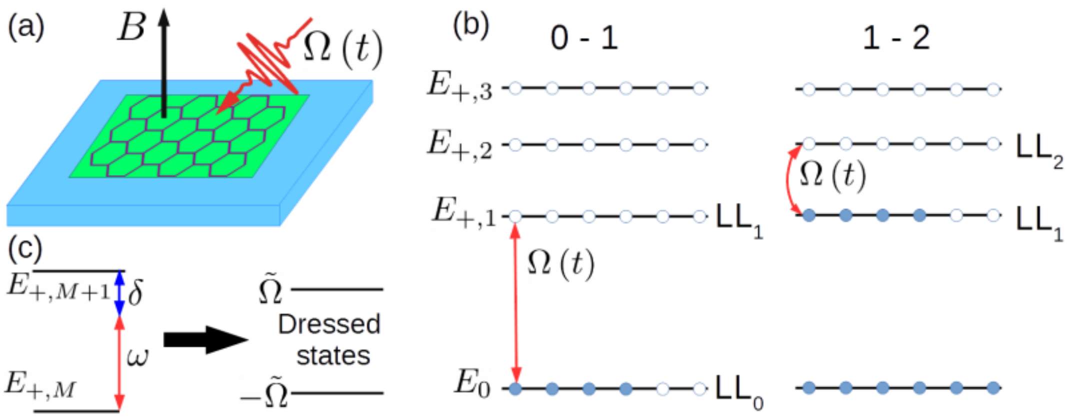

Depending on properties of the light, the orbital quantum number *m* is changed or not.

Symmetric gauge: *m* ↔ orbital angular momentum
Landau gauge: *m* ↔ momentum

LL gap

Coupling

$$H_0(t) = \sum_m \left[\frac{\Delta E}{2} \left(c^\dagger_{n+1,m} c_{n+1,m} - c^\dagger_{n,m} c_{n,m} \right) + \hbar\Omega \left(c^\dagger_{n+1,m+\mu} c_{n,m} \mathrm{e}^{-i(\Delta E - \delta)t} + \mathrm{h.c.} \right) \right.$$

Areg Ghazaryan, Michael J. Gullans, Pouyan Ghaemi, Mohammad Hafezi, *Light-induced fractional quantum Hall phases in graphene* (arXiv:1612.08748)

Optical coupling of graphene Landau levels

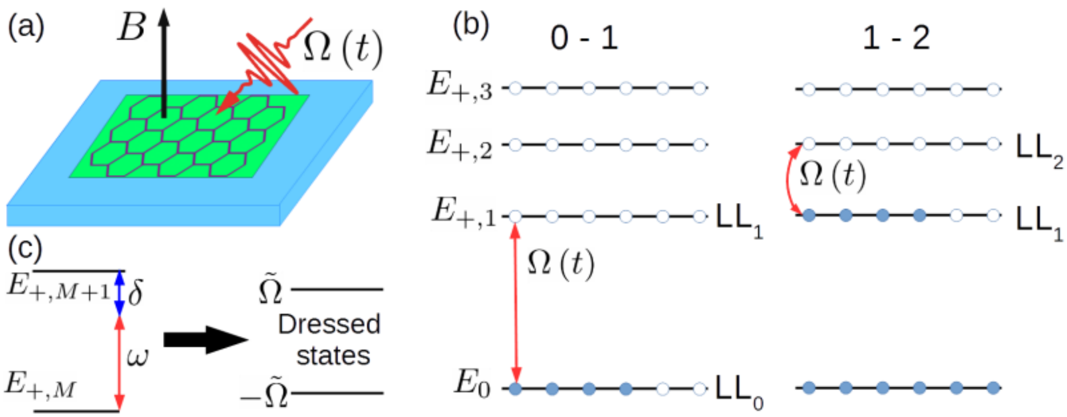

Depending on properties of the light, the orbital quantum number *m* is changed or not.

Symmetric gauge: *m* ↔ orbital angular momentum
Landau gauge: *m* ↔ momentum

LL gap

Coupling

$$H_0(t) = \sum_m \left[\frac{\Delta E}{2} \left(c^\dagger_{n+1,m} c_{n+1,m} - c^\dagger_{n,m} c_{n,m} \right) + \hbar\Omega \left(c^\dagger_{n+1,m+\mu} c_{n,m} \mathrm{e}^{-i(\Delta E - \delta)t} + \mathrm{h.c.} \right) \right.$$

In rotating frame after rotating wave approximation (RWA):

$$H_0 = \sum_m \left(\hbar\Omega c^\dagger_{n+1,m+\mu} c_{n,m} + \mathrm{h.c.} + \hbar\delta c^\dagger_{n+1,m} c_{n+1,m} \right)$$

Interactions after RWA:

$$V^{n_1,n_2,n_3,n_4 (\mathrm{RWA})}_{m_1,m_2,m_3,m_4} = \delta_{n_1+n_2-n_3-n_4} V^{n_1,n_2,n_3,n_4}_{m_1,m_2,m_3,m_4}$$

Tunable Fractional Quantum Hall Hamiltonian
(assuming spin and valley polarization):

$$H = H_0 + V^{(\mathrm{RWA})}$$

Areg Ghazaryan, Michael J. Gullans, Pouyan Ghaemi, Mohammad Hafezi, *Light-induced fractional quantum Hall phases in graphene* (arXiv:1612.08748)

Optical coupling of graphene Landau levels

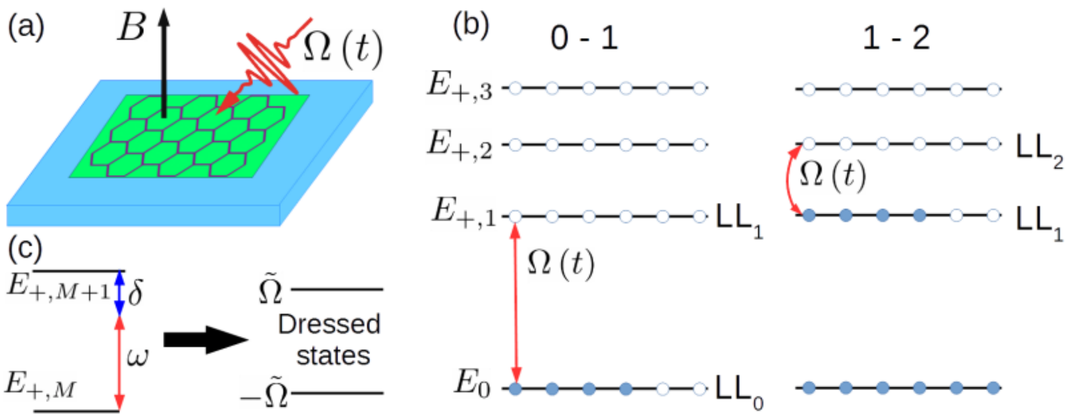

Three scenarios (all work in progress):

Strong coupling

Low-energy manifold: lower dressed Landau level.

How does dressing modify interactions?

Weak coupling

Both Landau levels can be occupied.

Bilayer quantum Hall phases?

Pulsed coupling

System is prepared in the lower level.

Transfer between Landau levels?

Strong coupling: Haldane pseudopotentials

$$V^{n_1 n_2, n_3 n_4}_{m_1 m_2, m_3 m_4} = \sum_{m,M} V^{n_1 n_2, n_3 n_4}_{m} P^{m_1 m_2}_{mM} P^{m_3 m_4}_{mM}$$

Dressed Landau level: $|s,m\rangle = \cos[\theta(\delta,\Omega)]|n+1,m+1\rangle + \sin[\theta(\delta,\Omega)]|n,m\rangle$

LL0 ↔ LL1

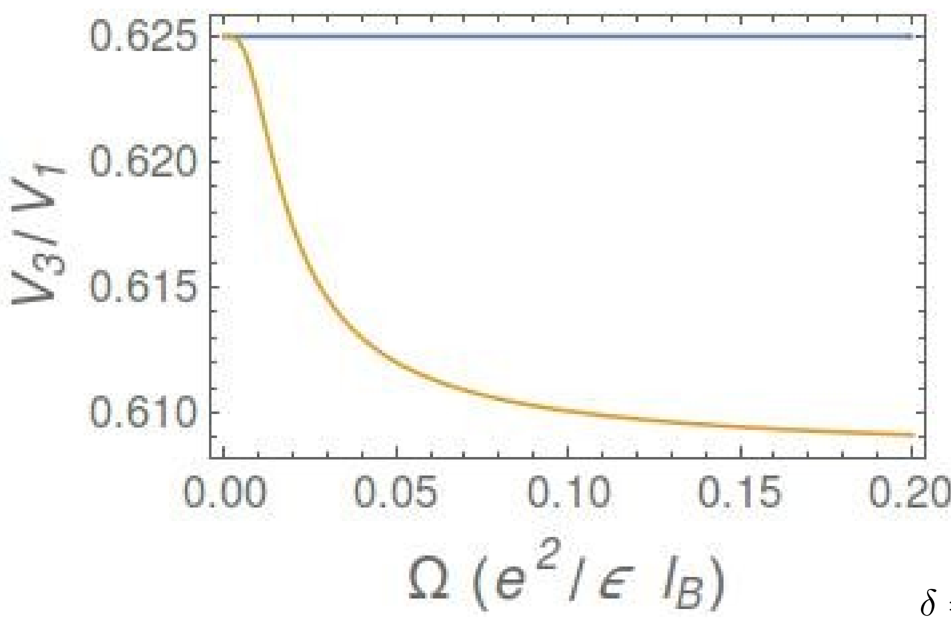

LL1 ↔ LL2

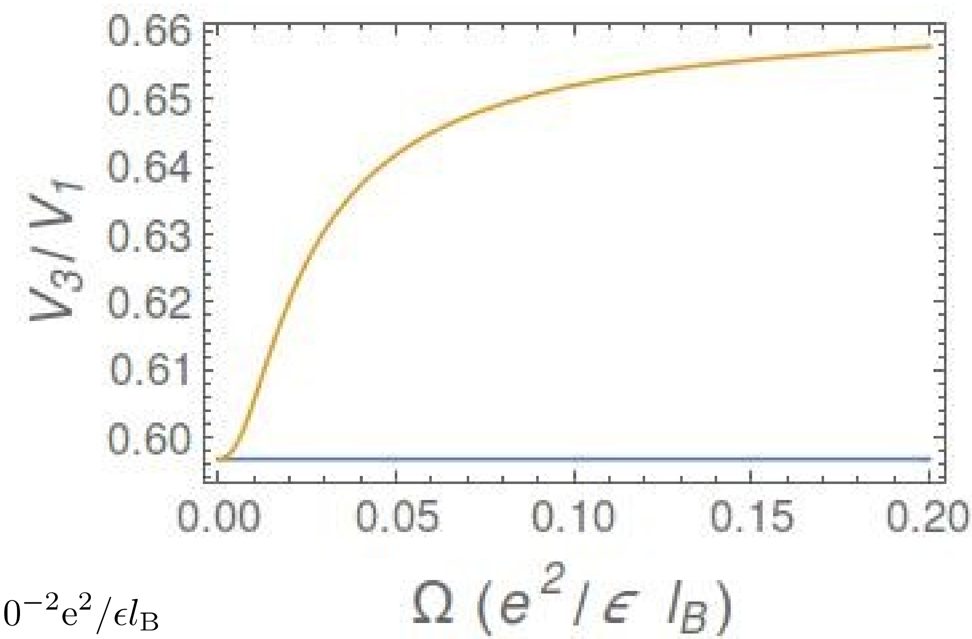

$\delta = 10^{-2} \mathrm{e}^2/\epsilon l_{\mathrm{B}}$

Modification of pseudopotentials are rather small.

We checked at filling ν=2/3 that strongly coupled system forms a PH-conjugated Laughlin phase, just as the uncoupled system does.

Effects at other filling factors?

Weak coupling: bilayer quantum Hall phases

Yrast line for coupling $\{2, m\} \leftrightarrow \{1, m\}$ $(N = 6, \Omega = 0.001, \delta = 0.02)$

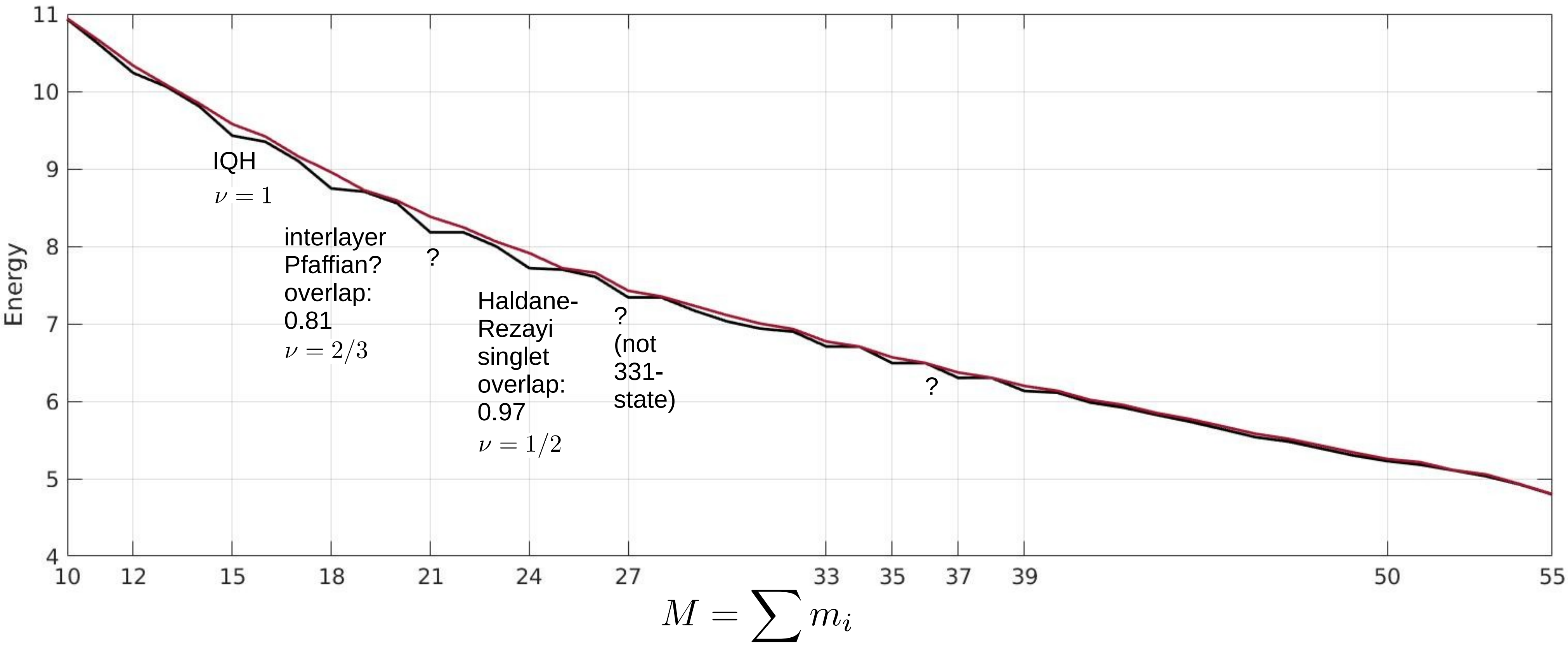

Competitors: *M=18* IR-Pfaffian vs. 330-state (both *v*=2/3)
M=24 HR state vs. Jain singlet (*v*=1/2 and *v*=2/3)

Weak coupling: bilayer quantum Hall phases

Many competing quantum Hall states at ν=2/3:

	Layer polarization	*Quasiparticles*	*Torus degeneracy*
PH Laughlin	Mono-layer	Abelian	3
$\mathbb{Z}_4$ (Read-Rezayi)	Mono-layer	Non-Abelian	15
330-Halperin	Singlet/bilayer	Abelian	9
112-Halperin	Singlet/bilayer	Abelian	3
CF (Jain)	Singlet/bilayer	Abelian	3
Interlayer Pfaffian	Singlet/bilayer	Non-Abelian	9
Intralayer Pfaffian	Singlet/bilayer	Non-Abelian	27
Fibonacci	Singlet/bilayer	Non-Abelian	6

PHYSICAL REVIEW B
covering condensed matter and materials physics

Highlights Recent Accepted Authors Referees Search Press About

Non-Abelian two-component fractional quantum Hall states

Maissam Barkeshli and Xiao-Gang Wen
Phys. Rev. B **82**, 233301 – Published 2 December 2010

PHYSICAL REVIEW LETTERS

Highlights Recent Accepted Collections Authors Referees Search Press Ab

Fibonacci Anyons From Abelian Bilayer Quantum Hall States

Abolhassan Vaezi and Maissam Barkeshli
Phys. Rev. Lett. **113**, 236804 – Published 3 December 2014

PHYSICAL REVIEW B
covering condensed matter and materials physics

Highlights Recent Accepted Authors Referees Search P

Rapid Communication

Non-Abelian phases in two-component $\nu = 2/3$ fractional quantum Hall states: Emergence of Fibonacci anyons

Zhao Liu, Abolhassan Vaezi, Kyungmin Lee, and Eun-Ah Kim
Phys. Rev. B **92**, 081102(R) – Published 5 August 2015

PHYSICAL REVIEW B
covering condensed matter and materials physics

Highlights Recent Accepted Authors Referees Search Press About

Abelian and non-Abelian states in $\nu = 2/3$ bilayer fractional quantum Hall systems

Michael R. Peterson, Yang-Le Wu, Meng Cheng, Maissam Barkeshli, Zhenghan Wang, and Sankar Das Sarma
Phys. Rev. B **92**, 035103 – Published 2 July 2015

PHYSICAL REVIEW B
covering condensed matter and materials physics

Highlights Recent Accepted Authors Referees Searc

Competing Abelian and non-Abelian topological orders in $\nu = 1/3 + 1/3$ quantum Hall bilayers

Scott Geraedts, Michael P. Zaletel, Zlatko Papić, and Roger S. K. Mong
Phys. Rev. B **91**, 205139 – Published 27 May 2015

Some results on the torus ...

$$\nu = 2/3, N = 8, \Omega = 0.001, \delta = 0.02$$

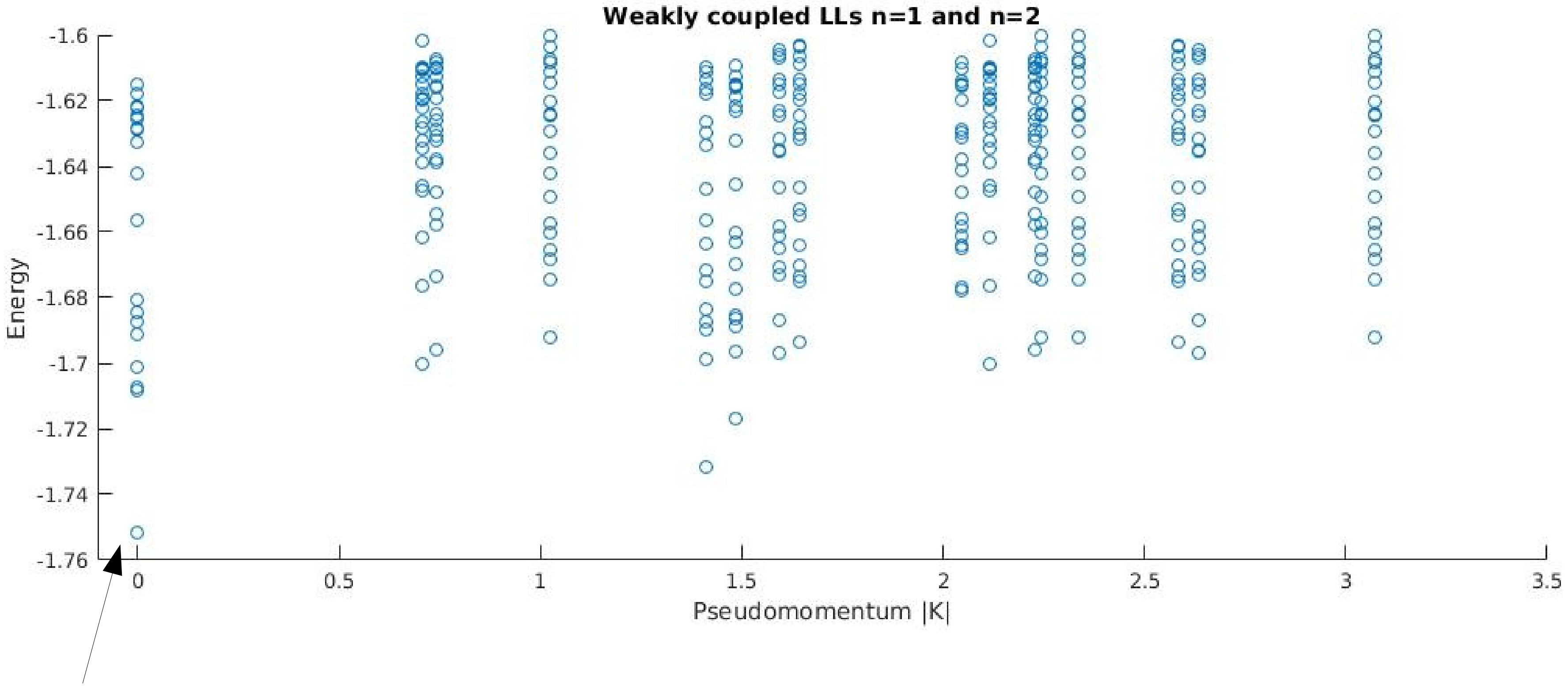

- 3-fold degenerate singlet
- but no good overlap with Jain state or 112-Halperin state
- Overlap with 330-state: 0.44

Some results on the torus ...

$\nu = 2/3, N = 8, \Omega \to 0, \delta = 0.02$

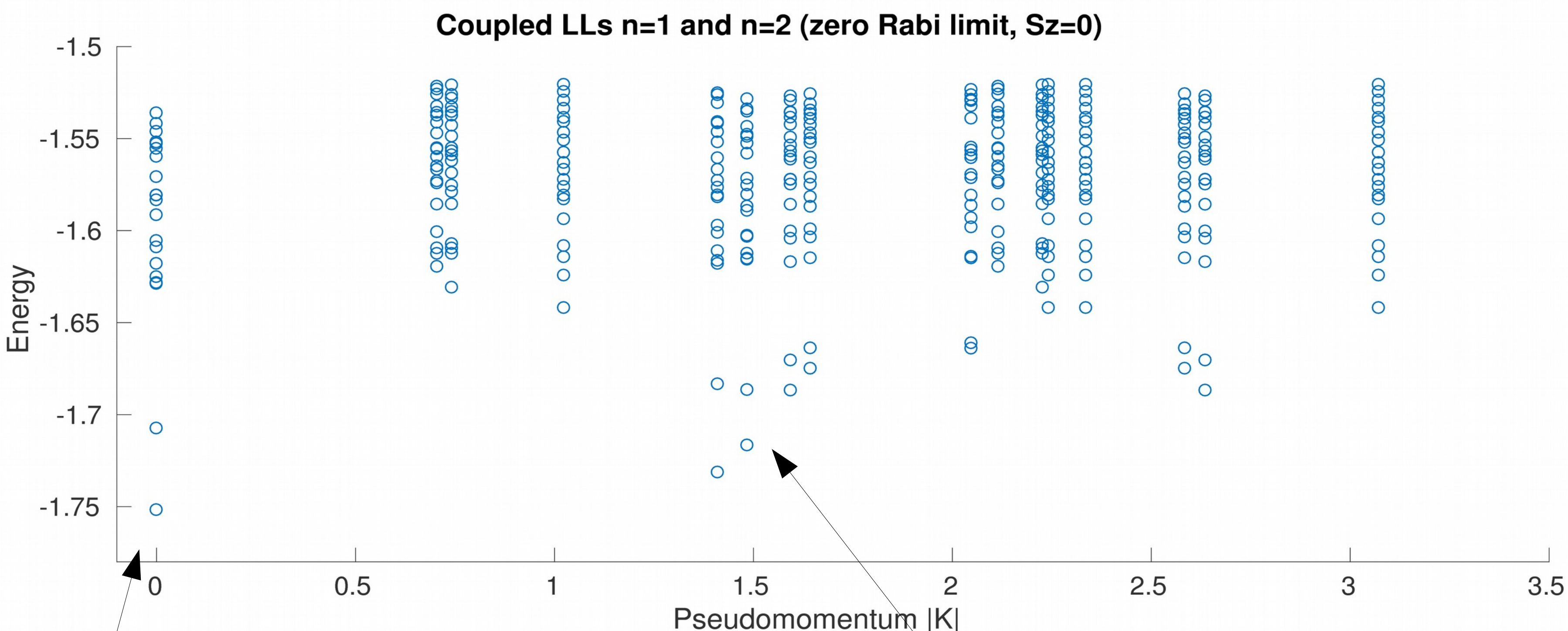

Roton instability?

Six-fold quasidegeneracy at *K*=0 ?
Fibonacci phase?

Some results on the torus ...

$\nu = 2/3, N = 10, \Omega = 0.001, \delta = 0.02$

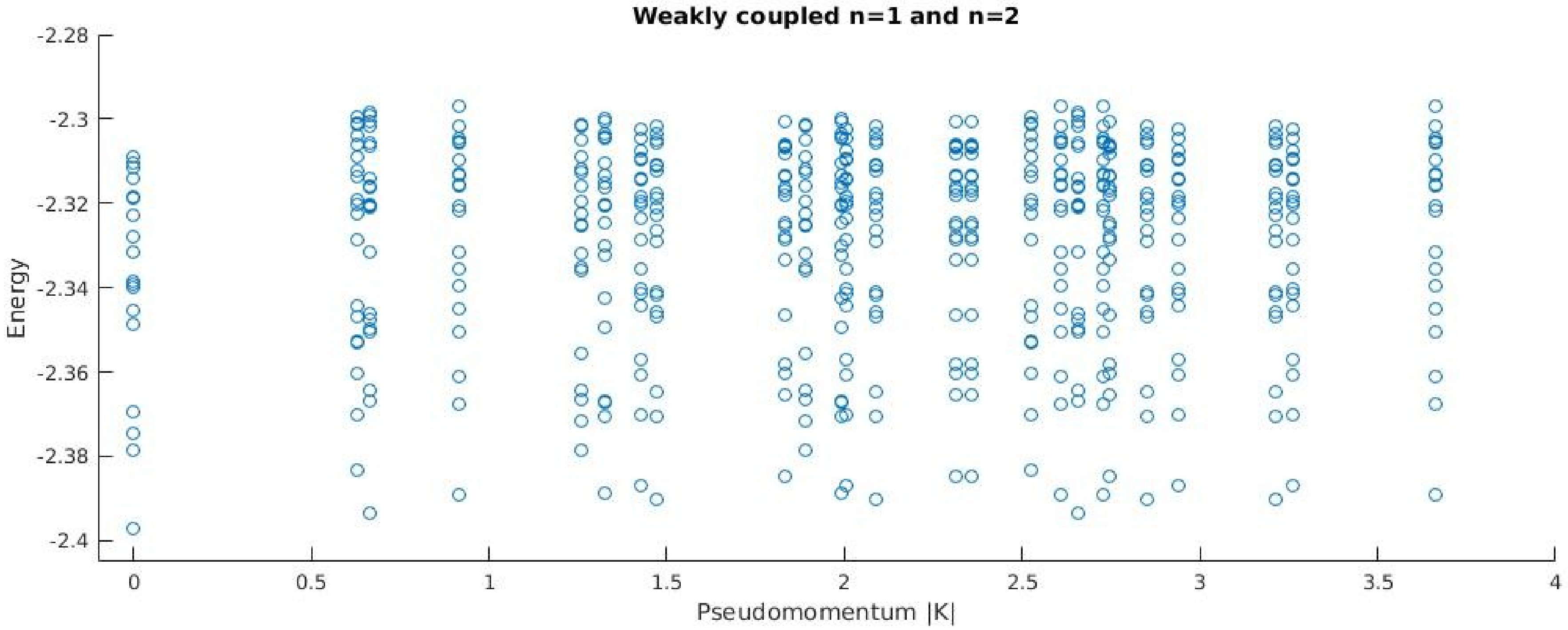

- No gap for N=10 → Compressible phase?
- Or is it an even/odd effect?
- Maybe interesting non-Abelian phases appear only in small systems?
- Or only for coupling with angular momentum exchange?

Coupling of two levels by a pulse

On the single-particle level, a π-pulse coupling “flips” the LL index:

$$\varphi_{n,m} \to \varphi_{n+1,m+1} = a^\dagger b^\dagger \varphi_{n,m}$$

Angular momentum is conserved here!

$$l = \hbar(m-n)$$

Does this also work on the many-body level?

$$\Psi \to \prod_{i=1}^{N} a_i^\dagger b_i^\dagger \Psi$$

This could be used to produce quasiholes:

$$\Psi = \Psi_{\mathrm{L}} \sim \prod_{i<j} (z_i - z_j)^3$$

Start with Laughlin state in LLL!

$$\left(\prod_i b_i^\dagger\right) \Psi \sim \left(\prod_i z_i\right) \Psi_{\mathrm{L}} \sim \Psi_{\mathrm{qh}}$$

Shift in *m*-quantum numbers produces quasihole!

$$\left(\prod_i a_i^\dagger\right) \Psi_{\mathrm{qh}} \sim \Psi'_{\mathrm{qh}}$$

Shift in *n*-quantum numbers translates state into higher Landau level!

Coupling of two levels by a pulse

On the single-particle level, a π-pulse coupling "flips" the LL index:

$$\varphi_{n,m} \to \varphi_{n+1,m+1} = a^\dagger b^\dagger \varphi_{n,m}$$

Does this also work on the many-body level?

$$\Psi \to \prod_{i=1}^{N} a_i^\dagger b_i^\dagger \Psi$$

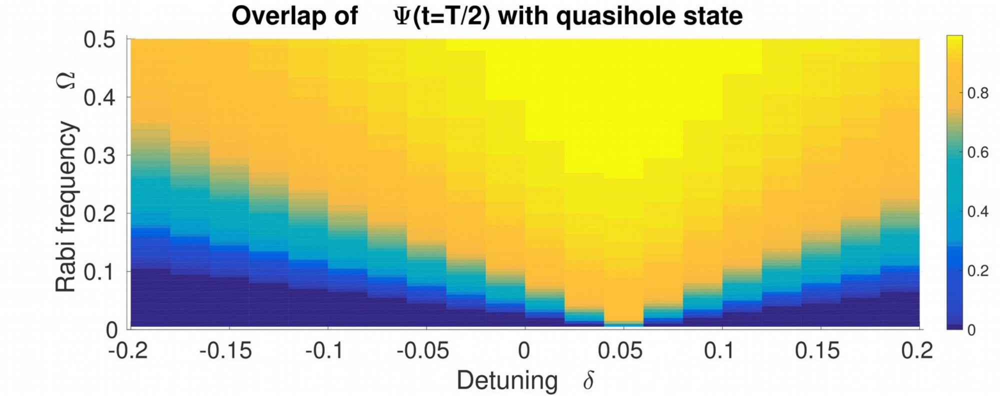

This could be used to produce quasiholes:

$$\Psi = \Psi_\mathrm{L} \sim \prod_{i<j} (z_i - z_j)^3$$

Start with Laughlin state in LLL!

$$\left(\prod_i b_i^\dagger\right) \Psi \sim \left(\prod_i z_i\right) \Psi_\mathrm{L} \sim \Psi_\mathrm{qh}$$

Shift in *m*-quantum numbers produces quasihole!

$$\left(\prod_i a_i^\dagger\right) \Psi_\mathrm{qh} \sim \Psi'_\mathrm{qh}$$

Shift in *n*-quantum numbers translates state into higher Landau level!

Modeling the time evolution

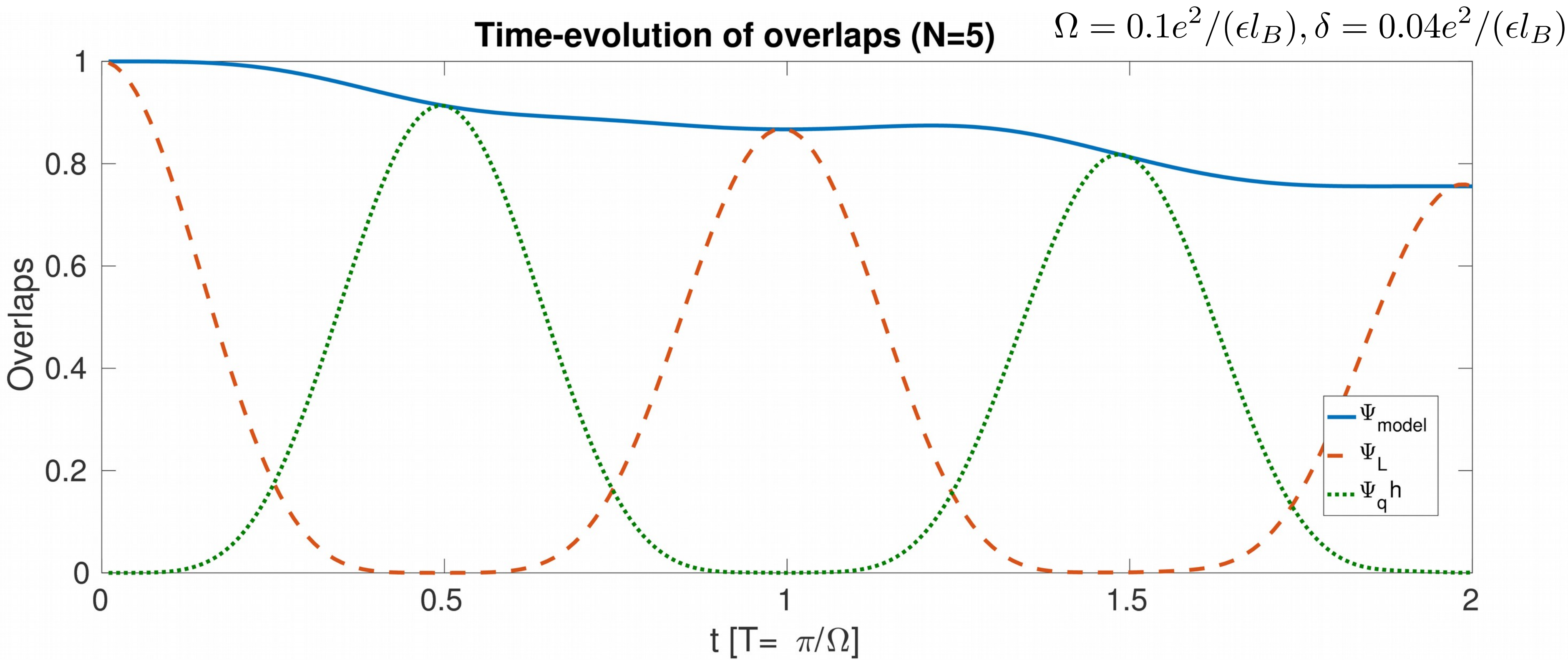

We model the wave function by superposition of **initial state**, **quasihole state**, and **edge-like excitations**:

$$\Psi_{\text{model}}(t) = \sum_{s=0}^{N} \sqrt{\binom{N}{s}} \cos(\Omega t)^{N-s} \sin(\Omega t)^s \Psi^{(s)},$$

$$\Psi^{(s)} = \sum_{\{k_1,\ldots,k_s\}} (-1)^{\sum_{j=1}^{s} k_j} (-i)^{\text{mod}(s,2)} \frac{1}{\sqrt{\binom{N}{s}}} \prod_{j=1}^{s} a^\dagger_{k_j} b^\dagger_{k_j} \Psi_{\text{L}}.$$

Measure fractional charge/statistics by interference of Laughlin and quasihole state?

[cf. proposal for atoms by Paredes, Fedichev, Cirac, Zoller, PRL 2001]

System is never in a superposition of only these two states.

Summary & Outlook

- Light can be used to control/ manipulate condensed matter
- Quantum Hall effect with graphene:
  Non-equidistant Landau levels → can selectively couple to two levels
- Different control scenarios are possible:

STRONG COUPLING

Engineer Haldane pseudopotentials!

WEAK COUPLING

Create new degree of freedom e.g. bilayer phases!

Maybe supporting non-Abelian anyons?

PULSED COUPLING

Create and braid quasiholes generated by light!

Thank you!